



## Novel Terpolymer Resin: Synthesis, Characterization and Ion-Exchange Studies of Terpolymer and its Composite

N. SIDHARAJ<sup>1</sup>, G. RAJARAJAN<sup>1,2,\*</sup> and M. SENTHIL<sup>3</sup>

<sup>1</sup>Department of Chemistry, Annamalai University, Chidambaram-608002, India

<sup>2</sup>Department of Chemistry, Bharathiar University, Coimbatore-641046, India

<sup>3</sup>Department of Chemistry, Kandaswami Kandar's College, Namakkal-638182, India

\*Corresponding author: E-mail: rajarajang70@gmail.com

Received: 9 July 2024;

Accepted: 12 August 2024;

Published online: 30 August 2024;

AJC-21745

A novel terpolymer containing biuret, 4,4'-oxydianiline and formaldehyde (BODF) was synthesized by condensation polymerization technique of biuret and 4,4'-oxydianiline with formaldehyde at different mole ratios (1:1:2) in dimethylformamide medium. The newly synthesized terpolymer was converted into its composite with chitosan. The terpolymer and its composite were characterized and confirmed by elemental analysis, FTIR, <sup>1</sup>H & <sup>13</sup>C NMR and UV-vis studies. The surface morphology of synthesized terpolymer resin with the incorporation of chitosan was examined by scanning electron microscopy (SEM). The chelation ion-exchange studies of synthesized terpolymer and its composite for the various metal ions were also carried out by batch equilibrium method under the estimation of metal ion uptake at different electrolytes and pH.

**Keywords:** 4,4'-Oxydianiline, Terpolymer composite, Batch equilibrium.

### INTRODUCTION

In worldwide, the major environmental pollution occurs from textile industries because of the release of disagreeable dye effluents. The variety of contaminants present in textile waste is harmful to live animals. Therefore, before discharging these effluents into receiving water channels, textile mills are typically mandated to treat them according to environmental legislation. Arsenic, cadmium, chromium, lead and mercury are some of the metals for public health because of their extreme toxicity [1-3].

The terpolymer ligand is understudied to be a cation exchanger between terpolymer and metal ions. The terpolymer ligand can be used selectively for the purification of wastewater [4]. Many researchers have extensively studied the ion exchange process of terpolymers. For some reactions are the ion exchange properties of copolymer resin derived from phthalic acid, thiosemicarbazide with formaldehyde terpolymer as reported by Thengane *et al.* [5]. Enhancing toxic metal ions and dye removal properties of diaminodiphenylmethane, resorcinol with formaldehyde terpolymer was reported by Vasanthakumar *et al.* [6]. The ion exchange applications of aminoacetophenone,

biuret with formaldehyde terpolymer reported by Rashid & Omran [7]. Similarly, Ahamed *et al.* [8] reported the sorption behaviour of ion-exchanger made up of 2-amino-6-nitrobenzothiazole, semicarbazide and formaldehyde terpolymer. The present communication is based on the comparatively ion exchange studies of terpolymer and its composite. The terpolymer ligand was derived from biuret, 4,4'-oxydianiline and formaldehyde (BODF). The novel BODF terpolymer was further converted into its composite with chitosan (BODFC). The synthesized novel BODF terpolymer and its composite was characterized in detail and also has been applied to remove heavy metal ions such as Cu<sup>2+</sup>, Pb<sup>2+</sup>, Zn<sup>2+</sup> and Cd<sup>2+</sup>.

### EXPERIMENTAL

Biuret was obtained from Sigma-Aldrich, whereas 4,4'-oxydianiline was purchased from Alfa Aesar. Formaldehyde and acetone (37%) were of AR grade and procured from Merck, India. Double distilled water was used for all the experiments. The other chemicals and reagents such as N,N-dimethylformamide, hydrochloric acid, sodium hydroxide and dimethyl sulfoxide were also of analytical grade and used without any further purification.

**Synthesis of terpolymer (BODF):** The terpolymer was synthesized by condensation polymerization method and utilizing DMF as response medium as well as catalyst. In brief, a mixture of biuret, 4,4'-oxydianiline, formaldehyde were taken in a 250 mL round bottom flask with refluxed in an oil bath at  $140 \pm 2$  °C for 6 h. After the reaction time to ensure equal mixing, the contents of the flask were occasionally vigorously shaken and poured into ice containing beaker with constant stirring and then left overnight. Residual monomers were eliminated by filtering and rinsing the product with hot water and methanol. The resin was then refined by being dissolved in a 1:1 hydrochloric acid/H<sub>2</sub>O solution and then being regenerated with 10% NaOH. The resin sample was eventually sorted into homogeneous 100 mesh-sized particles and kept in polyethylene bottle [9,10].

**Synthesis of terpolymer composite (BODFC):** In 1:1 ratio, BODF terpolymer and chitosan were utilized to prepare the terpolymer/chitosan composite. In order to get a transparent chitosan solution, 1 g of chitosan was first disintegrated in 2 M acetic acid and agitated for 0.5 h. The chitosan solution was then mixed to 1g of above prepared terpolmer resin while stirring continuously for 4 h at room temperature. Following the sufficient time, the obtained composite was filtered and dried for 24 h at 70 °C in oven (Scheme-I).

## RESULTS AND DISCUSSION

The terpolymer was soluble in conc. HCl, dimethyl formamide, tetrahydrofuran, HNO<sub>3</sub> and DMSO. Some mineral acids

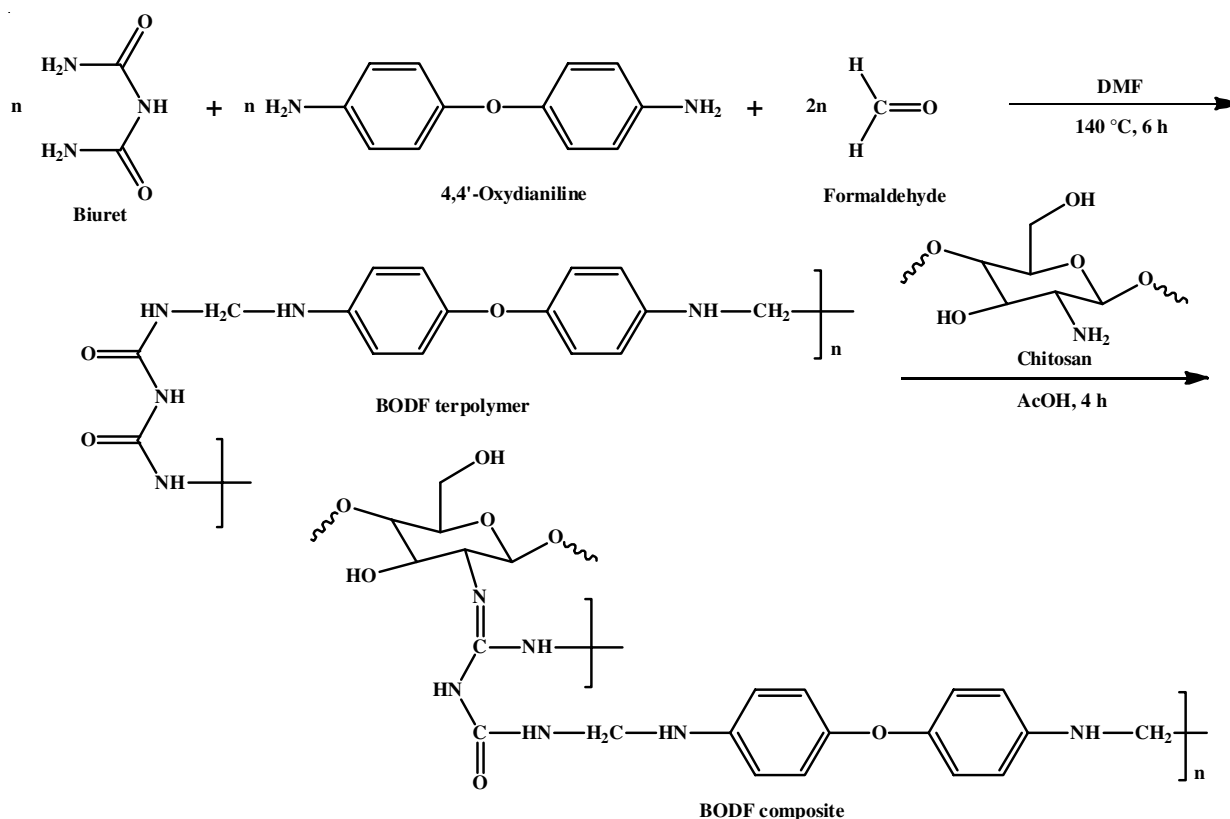
were somewhat soluble in the compound, but the terpolymer composite was soluble in DMSO solvent.

The percentage of elements such as C, H, O and N present in the terpolymer resin was determined using Elemental instrument Model Vario EL II. The C<sub>16</sub>H<sub>17</sub>N<sub>5</sub>O<sub>3</sub> was formed by the elements present in the repeating unit's terpolymer ligand formula. According to formula the percentages of calculated and experimental values of synthesized terpolymer elements such as carbon, hydrogen, nitrogen and oxygen were 58.71 (58.72), 5.19 (5.20), 21.40 (21.40) and 14.67 (14.68), respectively.

## Spectral studies of terpolymer and its composite

**FTIR studies:** The Fourier transform infrared spectrum of BODF terpolymer and its composite was scanned using the KBr pellet method on a Shimadzu model spectrometer and the resulting spectrum is shown in Fig. 1 and the key IR bands are shown in Table-1. The BODF terpolymer (Fig. 1a) spectrum showed that a broad band appeared in the range of 3305 cm<sup>-1</sup>, which is due to the -NH stretching mode of oxydianiline ether [11]. A weak band at 2916 cm<sup>-1</sup> indicates the existence of methylene group inside the terpolymer chain [12]. A sharp band present at 1624 cm<sup>-1</sup> is due to the carbonyl group of biuret, while a normal peak at 1494 cm<sup>-1</sup> is identified by C-C linkage in aromatic rings [13,14]. A strong peak obtained at 1236 cm<sup>-1</sup> may be assigned to the (C-O-C) ether group in the chain [15] and the occurrence of a medium band at 826 cm<sup>-1</sup> for an aromatic biphenyl ring [16].

Fig. 1b shows the FTIR spectrum of the BODF composite, which illustrates that there was a slight difference between



Scheme-I: Synthesis route of BODF terpolymer and its composite

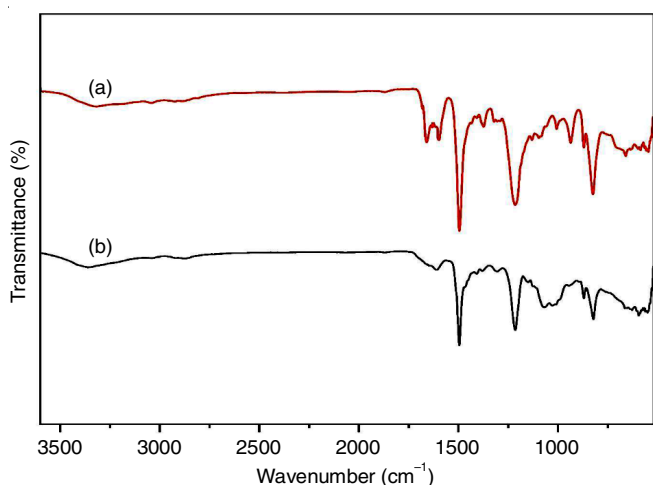


Fig. 1. FTIR spectrum of BODF terpolymer (a) and its composite (b)

TABLE-1  
FTIR DATA OF BODF TERPOLYMER  
AND ITS COMPOSITE (BODFC)

Mode of vibrations	Frequency (cm <sup>-1</sup> )	
	BODF	BODFC
-NH stretching in oxydianiline ring	3305.2	3347.0
-CH <sub>2</sub> chain in terpolymer	2916.3	2870.9
-CO group of biuret	1624.9	-
C=N attachment	-	1612.1
C-C stretching in aromatic ring	1494.6	1494.3
C-O-C stretching (ether)	1236.1	1220.6
Aromatic biphenyl ring	826.5	820.5

the composite and terpolymer spectrums. A broad peak at 3347 cm<sup>-1</sup> was represented as a -NH stretching mode of the BODF composite and it has shifted from the terpolymer absorption, which clearly confirmed the formation of the composite. In other words, the presence of a -CH<sub>2</sub> stretch was indicated by a weak band at 2870 cm<sup>-1</sup> in the composite chain. The medium band at 1612 cm<sup>-1</sup> indicated to C=N attachment of the BODF composite. The terpolymer engagement with chitosan was further confirmed by appearance of various band absorptions and the lowered absorption band values. According to the analyses aforesaid, the terpolymer and chitosan successfully formed the composite [17,18].

**<sup>1</sup>H NMR spectral studies:** The NMR (<sup>1</sup>H and <sup>13</sup>C) spectra of the terpolymer recorded using deuterated dimethylsulfoxide

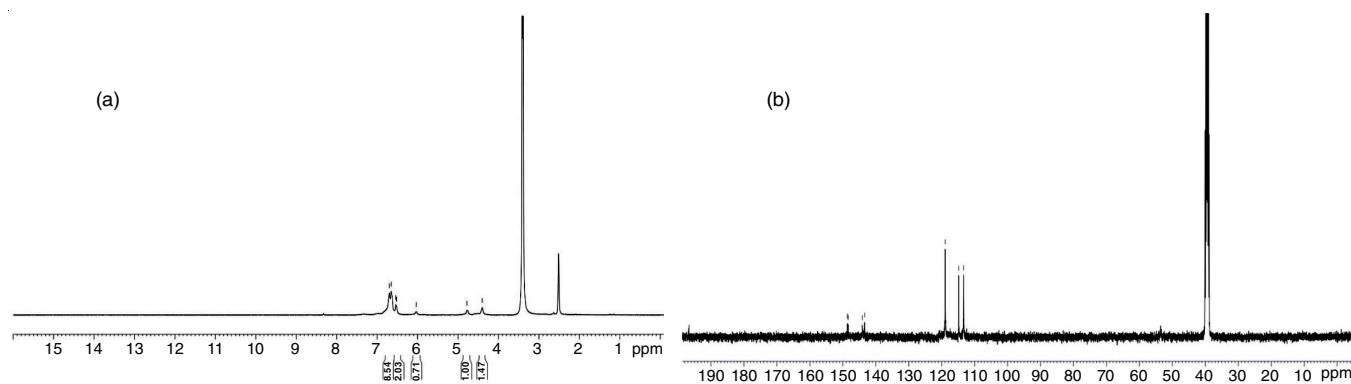
(DMSO) as a solvent. From the spectrum (Fig. 2a), the multiple signals appeared in the range at δ 6.0-6.6 ppm are attributed to the aromatic ring [19,20]. In the region δ 4.7 ppm of the spectrum is represented to CO-NH group present in terpolymer. The peak in the spectrum at δ 4.4 ppm is attributed to the NH group of oxydianiline. The weak signal at δ 2.5 ppm could be due to the methylene proton of the -CH<sub>2</sub> bond [21-23].

**<sup>13</sup>C NMR spectral studies:** The <sup>13</sup>C NMR spectrum of BODF terpolymer is depicted in Fig. 2b. The corresponding peaks displayed at δ 111.34, 114.81, 118.88, 143.36 and 144.03 ppm are indicative of the presence of an aromatic carbon terpolymer. The chemical shift formed at δ 148.34 and 148.59 ppm is due to the NH-CO group [24].

**Electronic spectra:** In Fig. 3, the UV-Vis spectra of BODF terpolymer (Fig. 3a) and its composite (BODFC) (Fig. 3b) were altered. The UV spectra of BODF terpolymer consist of two absorption bands at 283 nm and 340 nm. The aromatic ring in the terpolymer designated for the π-π\* transition may be responsible for the band observed at 283 nm. The band at 340 nm was attributed to the terpolymer >NH group's presence in the n-π\* transition. This n-π\* electronic forbidden transition has a longer wavelength and a less intense band that move towards the redshift or bathochromic shift [25].

As shown in Fig. 3b, the composite exhibited four bands situated at 220 nm, 290 nm, 345 nm and 390 nm, which correspond to π-π\* and n-π\* transitions. The two bands were observed at 220 nm and 290 nm, respectively, which may be attributed to the π-π\*, the allowed transition of conjugation in the two different aromatic rings in the terpolymer backbone. The π-π\* transition could be identified as a more intense band with a shorter wavelength that moves toward a blue shift or hypsochromic shift. The third and fourth absorption bands were observed at 345 nm and 390 nm, which were caused by n-π\* transition of the >NH group in composite. The results provided confirm that the shifting of bands caused the composite to form. Furthermore, it clearly favours composite formation because the absorption band is smaller when compared to terpolymer.

**Morphology studies:** The surface morphology of the synthesized BODF terpolymer and its composite were observed using 500X magnification scanning electron micrographs (Fig. 4). These images show deeper pits, strong cracks and ruggedness on the surface, which indicates the polycrystalline nature of the sample. The crystalline nature may be due to the basic

Fig. 2. <sup>1</sup>H NMR (a) and <sup>13</sup>C NMR (b) spectrum of BODF terpolymer ligand

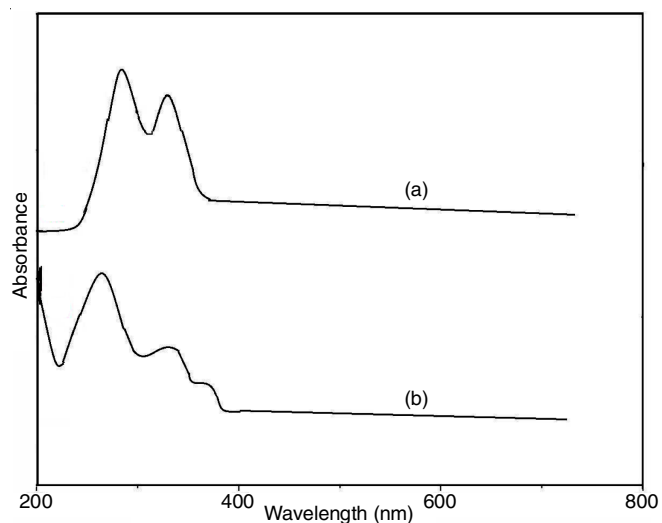


Fig. 3. UV-Vis spectra of BODF terpolymer (a) and its composite (b)

nature of the monomers. The BODF terpolymer appears to be hard, rigid, less tightly packed and highly rough on the surface

helps in increasing the sorption of metal ions due to the high affinity of the terpolymer resin for the metal ions.

The surface morphology of terpolymer composite (Fig. 4b) illustrates that its surface morphology is dissimilar from that of terpolymer. It has a rough surface and varied surface apertures when compared to the terpolymer. Also, it could be found that the composite has a porous structure, thus mass ion exchange transfer can play a crucial function in the extraction and adsorption processes. Additionally, the composite possesses more voids due to its increased surface area. Based on the above analyses, the composite would have a higher chance of showing a superior ion exchanger than the terpolymer. The SEM study proved that the composite was formed perfectly.

#### Ion-exchange studies

**Metal ion uptake in different electrolytes:** The chelating ion-exchange capacity of BODF terpolymer and its composite was determined using the batch equilibrium technique against  $\text{Cu}^{2+}$ ,  $\text{Zn}^{2+}$ ,  $\text{Pb}^{2+}$  and  $\text{Cd}^{2+}$  ions in different electrolytes, namely NaCl,  $\text{NaNO}_3$  and  $\text{Na}_2\text{SO}_4$  with varying concentrations of 0.1, 0.5 and 1.0 M. According to the observed data (Table-2), the

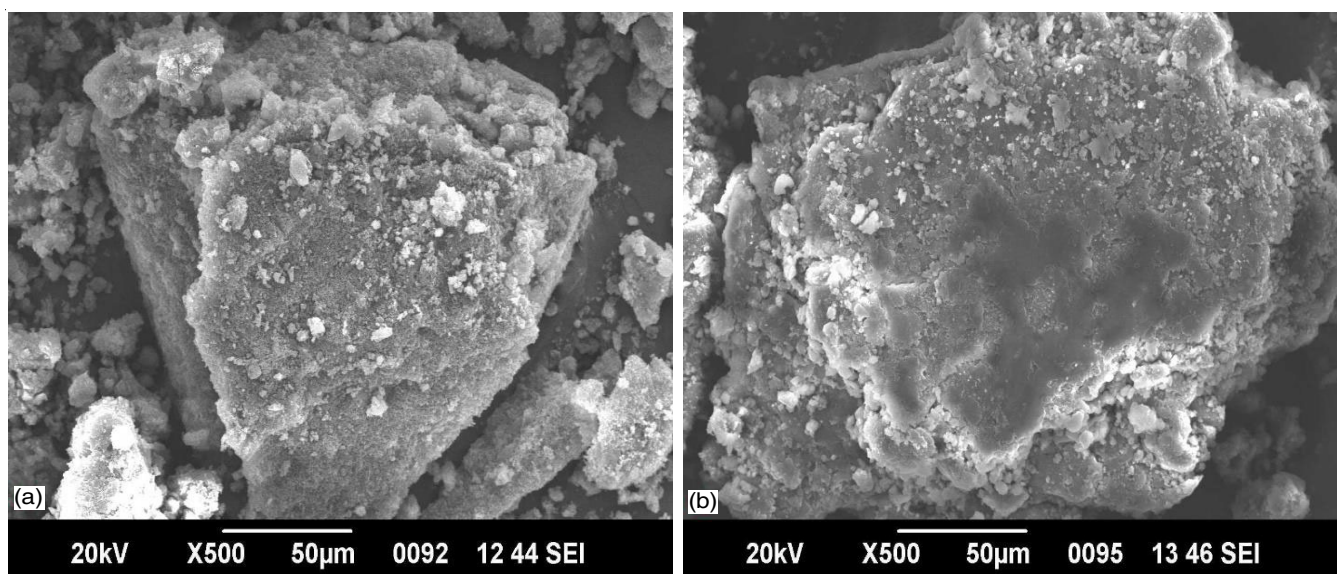


Fig. 4. SEM image of BODF terpolymer (a) and its composite (b)

TABLE-2  
EFFECT OF METAL ION UPTAKE BY BODF TERPOLYMER & COMPOSITE

Metal ions	Conc. of electrolytes (mol L <sup>-1</sup> )	Metal ion uptake in the presence of electrolytes (mmol/g)					
		NaCl		NaNO <sub>3</sub>		Na <sub>2</sub> SO <sub>4</sub>	
		BODF	BODFC	BODF	BODFC	BODF	BODFC
Cu <sup>2+</sup>	0.1	4.28	5.46	4.37	5.13	1.28	2.37
	0.5	6.49	7.12	5.49	6.06	2.15	3.41
	1.0	7.10	8.25	6.56	7.35	2.88	4.58
Zn <sup>2+</sup>	0.1	3.56	4.62	3.42	4.73	1.20	2.79
	0.5	4.35	5.74	4.37	5.38	1.43	3.02
	1.0	5.68	6.09	4.63	5.79	1.92	3.95
Cd <sup>2+</sup>	0.1	2.51	3.39	2.58	3.12	0.91	1.86
	0.5	3.67	4.16	3.37	4.03	1.33	2.59
	1.0	4.19	5.28	3.83	4.70	1.86	2.05
Pb <sup>2+</sup>	0.1	3.32	4.20	3.15	3.98	1.12	2.76
	0.5	3.94	5.13	4.09	4.79	1.39	2.94
	1.0	4.45	5.75	4.23	5.25	1.83	2.80



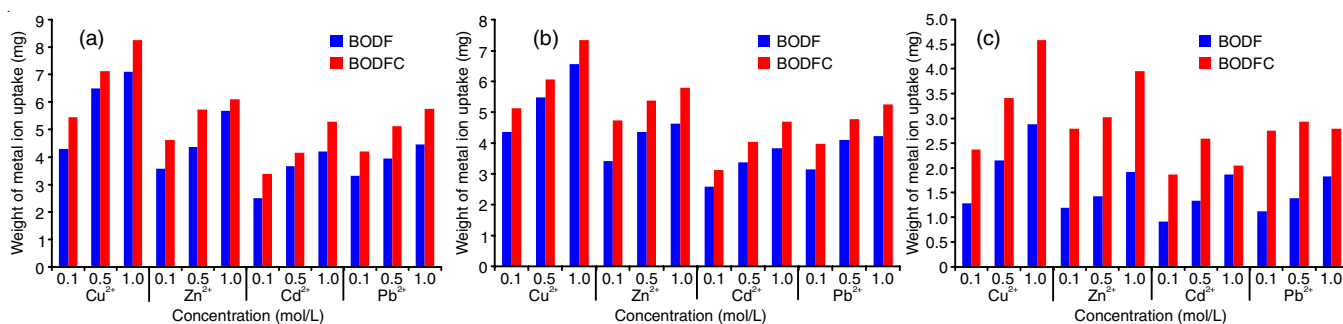


Fig. 5. Effect of NaCl (a), NaNO<sub>3</sub> (b) and Na<sub>2</sub>SO<sub>4</sub> (c) electrolyte on metal ion uptake by BODF terpolymer and its composite

rate of metal ion uptake by a specific amount of terpolymer resin changes with the electrolyte concentration. The amount of metal ion uptake by the terpolymer resin increases with rising Cl<sup>-</sup> concentration and decreases with increasing NO<sub>3</sub><sup>-</sup> concentration. The reason are that due to forming strong chelates with metal ions, the effect of dissimilar Cl<sup>-</sup> and NO<sub>3</sub><sup>-</sup> ion concentrations on metal chelate equilibrium.

The amount of Cu<sup>2+</sup> and Zn<sup>2+</sup> ions uptake by the BODF terpolymer is comparatively higher than the other metal ions, which might be owing to the poor chelation of Pb<sup>2+</sup> and Cd<sup>2+</sup> ions with the electrolyte anions. In addition, the structure of the terpolymer surface is highly porous, thus it readily accommodates metal ions and functions as an efficient ion-exchanger. The good ion exchange capacity of both terpolymer resin and its composite may be due to the presence of -NH group in the terpolymer structure and the metal ions uptake difference are clearly seen in Fig. 5. The selectivity of the BODF terpolymer and its composite was determined to be Cu<sup>2+</sup> > Zn<sup>2+</sup> > Pb<sup>2+</sup> > Cd<sup>2+</sup>.

By using the batch separation method, a comparison of the influence of metal ion uptake by the terpolymer and its composites was also evaluated. Owing to its expanded surface area and the existence of porosity, the BODF composite has a higher metal ions uptake capacity than the BODF terpolymer. This might be caused by the metal ions' differing stability constant and pore size.

**Variation of metal ions uptake at different pHs:** The distribution of selected metal ions such as Cu<sup>2+</sup>, Pb<sup>2+</sup>, Zn<sup>2+</sup> and Cd<sup>2+</sup> between the polymer phase and aqueous phase was evaluated at room temperature in the presence of 1 M KNO<sub>3</sub> throughout a pH range of 1.5 to 6.0. It was found that the equilibrium rate of metal ion uptake by BODF terpolymer and its composite increases with increasing pHs (Fig. 6). It is expected that the equilibrium state will be reached after 24 h at 25 °C. The terpolymer absorbs Cu<sup>2+</sup> ions more efficiently as compared to other studied metals ions under all pH conditions. Furthermore, for the entire pHs range, Pb<sup>2+</sup> and Zn<sup>2+</sup> ions have a medium representation ratio, whereas Cd<sup>2+</sup> has a lower ratio. This can be explained by the formation of a metal complex resulting from the reduced stabilization energy of metal ions. Moreover, the decreasing order of distribution ratio of the metal ions is found to be Cu<sup>2+</sup> > Zn<sup>2+</sup> > Pb<sup>2+</sup> > Cd<sup>2+</sup>.

## Conclusion

The BODF terpolymer was synthesized from biuret and 4,4'-oxydianiline with formaldehyde in the presence of DMF

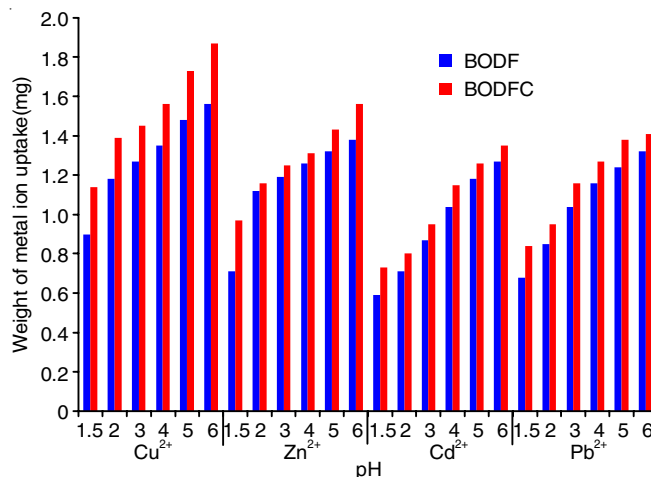


Fig. 6. Metal ion uptake by BODF terpolymer and its composite at different pH

by condensation polymerization. Then the prepared terpolymer was converted into its composite by reaction with chitosan. Based on the FTIR and UV spectral data, the formation of BODF terpolymer and its composite were confirmed. The NMR study showed the proton and carbon existing in the terpolymer. From the SEM images confirmed that the terpolymer and composite were polycrystalline in nature. The batch equilibrium studies of terpolymer and its composite were examined at different pHs and electrolytes. The chelation ion-exchange studies displayed that the terpolymer can act as an effective ion exchanger for various divalent metal ions such as Cu<sup>2+</sup>, Pb<sup>2+</sup>, Zn<sup>2+</sup> and Cd<sup>2+</sup>. The amount of Cu<sup>2+</sup> metal ions uptake by the synthesized terpolymer and its composite were comparatively higher than that of the other metal ions such as Pb<sup>2+</sup>, Zn<sup>2+</sup> and Cd<sup>2+</sup>. The BODF terpolymer and composite were also shown to have selectivity in the following order: Cu<sup>2+</sup> > Zn<sup>2+</sup> > Pb<sup>2+</sup> > Cd<sup>2+</sup>.

## ACKNOWLEDGEMENTS

The authors are thankful to the Head of the Department of Chemistry, Annamalai University, Chidambaram, India, for providing the necessary research facilities.

## CONFLICT OF INTEREST

The authors declare that there is no conflict of interests regarding the publication of this article.

## REFERENCES

1. B. Lellis, C.Z. Favaro-Polonio, J.A. Pamphile and J.C. Polonio, *Biotechnol. Res. Innov.*, **3**, 275 (2019); <https://doi.org/10.1016/j.biori.2019.09.001>
2. D.A. Yaseen and M. Scholz, *Int. J. Environ. Sci. Technol.*, **16**, 1193 (2019); <https://doi.org/10.1007/s13762-018-2130-z>
3. S. Velusamy, A. Roy, S. Sundaram and T. Kumar Mallick, *Chem. Rec.*, **21**, 1570 (2021); <https://doi.org/10.1002/tcr.202000153>
4. B. Sabitha, B.S. Rao, B.C. Mouli and R. Sharma, *Mater. Today Proc.*, **64**, 64 (2022); <https://doi.org/10.1016/j.matpr.2022.03.664>
5. R. Thengane, J.V. Khobragade and W.B. Gurnule, *Int. J. Res. Biosci. Agric. Technol.*, **2**, 256 (2023); <http://doi.org/10.29369/ijrbat.2023.02.1.0037>
6. V. Vasanthakumar, A. Priyadharsan, P.M. Anbarasan, S. Muthumari, S. Subramanian and V. Raj, *ChemistrySelect*, **2**, 9501 (2017); <https://doi.org/10.1002/slct.201700685>
7. A.K. Rashid and K.A. Omran, *Asian J. Chem.*, **29**, 2419 (2017); <https://doi.org/10.14233/ajchem.2017.20721>
8. M.A.R. Ahamed, R.S. Azarudeen, R. Subha and A.R. Burkanudeen, *Polym. Bull.*, **71**, 3209 (2014); <https://doi.org/10.1007/s00289-014-1246-7>
9. V. Bhadja, U. Chatterjee and S.K. Jewrajke, *RSC Adv.*, **5**, 40026 (2015); <https://doi.org/10.1039/C5RA07191G>
10. S.D. Kudade, S.K. Singh, P.V. Tekade, R.R. Naik and S.V. Bawankar, *New J. Chem.*, **40**, 705 (2016); <https://doi.org/10.1039/C5NJ02184G>
11. V. Vasanthakumar, A. Saranya, A. Raja, S. Prakash, V. Anbarasu, P. Priya and V. Raj, *RSC Adv.*, **6**, 54904 (2016); <https://doi.org/10.1039/C6RA05115D>
12. D. Li and M. Liao, *J. Fluorine Chem.*, **201**, 55 (2017); <https://doi.org/10.1016/j.jfluchem.2017.08.002>
13. D.B. Patle and W.B. Gurnule, *Arab. J. Chem.*, **9**, 648 (2016); <https://doi.org/10.1016/j.arabjc.2011.07.013>
14. E.Y. Calvillo-Munoz, A. Vega-Paz, D. Guzman-Lucero, I.V. Lijanova, O. Olivares-Xometl and N.V. Likhanova, *RSC Adv.*, **12**, 12273 (2022); <https://doi.org/10.1039/D2RA01173E>
15. X. Bian, S. Fan, G. Xia, J.H. Xin and S. Jiang, *J. Polym. Res.*, **31**, 192 (2024); <https://doi.org/10.1007/s10965-024-04024-1>
16. N.L. Bhandari, J. Ghimire, S. Shrestha, G. Bhandari, S. Bhattarai and R. Adhikari, *Asian J. Chem.*, **33**, 404 (2021); <https://doi.org/10.14233/ajchem.2021.23008>
17. I. Elganidi, B.S. Elarbe, N. Abdullah and N. Ridzuan, *IOP Conf. Ser.: Mater. Sci. Eng.*, **702**, 012027 (2019); <https://doi.org/10.1088/1757-899X/702/1/012027>
18. S. Shroff, P.P. Mohanta, I. Baitharu, B.P. Bag and A.K. Behera, *J. Serb. Chem. Soc.*, **87**, 813 (2022); <https://doi.org/10.2298/JSC210123031S>
19. S. Singh, N. Bahuguna, K. Singhal and P. Raj, *Asian J. Chem.*, **33**, 387 (2021); <https://doi.org/10.14233/ajchem.2021.23045>
20. D. Periyann and U. Chinnasamy, *Asian J. Chem.*, **33**, 459 (2021); <https://doi.org/10.14233/ajchem.2021.22549>
21. M.S. Dhore and A.B. Zade, *J. Eng. Technol.*, **2**, 33 (2013).
22. B.A. Shareef, I.F. Waheed and K.K. Jalaot, *Orient. J. Chem.*, **29**, 1391 (2013); <https://doi.org/10.13005/ojc/290414>
23. W.B. Gurnule, P.G. Gupta, R.H. Gupta, Y.U. Rathod and N.B. Singh, *IOP Conf. Ser.: Earth Environ. Sci.*, **1281**, 012026 (2023); <https://doi.org/10.1088/1755-1315/1281/1/012026>
24. A.J. Ahamed and N.M. Kani, *Int. J. Pharm. Chem.*, **5**, 359 (2015); <https://doi.org/10.7439/ijpc/5/359>
25. L. Feng and J.O. Iroh, *J. Chem. Appl.*, **1**, 1 (2022); [https://doi.org/10.47363/JCIA/2022\(1\)104](https://doi.org/10.47363/JCIA/2022(1)104)